Joint Estimation of Hemodynamic Response and Stimulus Function in Functional Ultrasound Using Convolutive Mixtures

Erol, Aybuke; Eyndhoven, Simon Van; Koekkoek, Sebastiaan; Kruizinga, Pieter; Hunyadi, Borbala

DOI
10.1109/IEEECONF51394.2020.9443299

Publication date
2020

Document Version
Final published version

Published in
2020 54th Asilomar Conference on Signals, Systems, and Computers

2020 54th Asilomar Conference on Signals, Systems, and Computers | 978-0-7381-3126-9/20/$31.00 ©2020 IEEE | DOI: 10.1109/IEEECONF51394.2020.9443299

JOINT ESTIMATION OF HEMODYNAMIC RESPONSE AND STIMULUS FUNCTION IN FUNCTIONAL ULTRASOUND USING CONVOLUTIVE MIXTURES

Aybüke Erol[1]*, Simon Van Eyndhoven*[2]*, Sebastiaan Koekkoek*[3]*, Pieter Kruizinga*[3] *and Borbala Hunyadi*[1]

[1]Circuits and Systems (CAS), Delft University of Technology, The Netherlands
[2]STADIUS Center for Dynamical Systems, Signal Processing and Data Analytics, KU Leuven, Belgium
[3]Department of Neuroscience - CUBE, Erasmus MC, The Netherlands

ABSTRACT

Functional ultrasound (fUS) is an exciting new neuroimaging technique that is able to record brain activity similar to functional magnetic resonance imaging, yet with higher spatiotemporal resolution and at lower cost. We consider the problem of jointly estimating the underlying neural sources and the hemodynamic response function (HRF) from fUS recordings. We propose to model the measured voxel time-series as a convolutive mixture of multiple source signals and solve the blind deconvolution problem via block-term decomposition. This allows us to estimate both the source time courses and a different HRF for each voxel and source combination, which accounts for the variability of HRF across different brain regions and events respectively. The proposed approach is proven to be robust against noise via simulations and further validated on real fUS data by performing a visual experiment on a mouse. The obtained results show that the proposed method is able to recover the timings of the visual paradigm.

***Index Terms*—** hemodynamic response function, neural activation, convolutive mixtures, functional ultrasound

1. INTRODUCTION

Functional ultrasound (fUS) is a novel neuroimaging modality that infers brain activity by measuring the changes in blood flow and volume. When a brain region becomes active, it demands an increased supply of oxygen-rich blood, resulting in a rise of blood flow to the region. This interaction between blood flow and metabolic activity is known as neurovascular coupling (NVC) whereas the associated changes in blood flow are referred as the hemodynamic response. When ultrasonic waves are transmitted to an imaging region, the changing number of moving red blood cells in response to neural activity directly affects the power of back-scattered waves. This way, fUS records the hemodynamic response of the brain, which gives an indirect measure of the underlying neural activity through NVC. In other words, similar to functional magnetic resonance imaging (fMRI), the strength of NVC in the local region determines the characteristics of the hemodynamic activity acquired with fUS [1].

Hemodynamic response is typically modeled as the output of a linear time-invariant (LTI) system. This model allows measurements to be characterized in terms of an impulse response, known as the hemodynamic response function (HRF). Correct prediction of HRF plays a crucial role in analysis and interpretation of the neuroimaging data, and there are several methods dedicated to this particular task in the fMRI literature. These methods can be categorized into four. In the first approach, an a priori shape of the HRF is assumed and only its amplitude, i.e. the activation level is of concern. This shape is mostly selected after the canonical HRF model, which was determined as a result of many empirical observations [2]. However, it is shown that not only the magnitude, but also parameters such as the time-to-peak and duration of HRF change significantly between subjects, brain regions and events [3]. Hence, assuming a constant shape for the HRF regardless of such variables, can result in misspecification of the HRF and mislead the estimation of brain activity. Therefore, in the second category, parameters that define the shape of the HRF are estimated as well. The third approach, known as the general linear model (GLM), expresses the HRF as a linear combination of several basis functions and attempts to find the optimum regression coefficients [4]. The fourth and final category makes no assumptions on the shape of the HRFs and predicts the value of the HRF separately at each time point, which increases the computational complexity and might result in arbitrary or physiologically meaningless shapes [5].

The HRF estimation methods described so far heavily rely on prior knowledge about the stimulus signal, which is quite commonly modeled as a binary vector based on the known onsets and durations within the experimental paradigm. However, such information may not always be available (for instance, resting state data) whereas its recovery remains of interest, as in cases where neural activity occurs spontaneously such as for epileptic seizure detection. Furthermore, if different stimulus conditions are incorporated during an experiment, such as a changing image contrast or odor concentration in visual and olfactory paradigms respectively, a binary on-off representation of the stimulus will not be enough to model the non-identical conditions [6]. As such, [7] and [8] estimate the stimulus signal by assuming a fixed HRF and do not take into account the variability of the HRF in different regions, subjects or events.

Following the significance of both problems, we consider joint estimation of the HRFs and stimulus signal. This issue has been addressed by [9] where the authors first find the time intervals in which the received hemodynamic signal shows activation by thresholding the data. The stimulus signal is expressed as an impulse train by predicting the optimal time lag between the possible stimulus spikes and the hemodynamic activity based on when the activation starts. Next, the unknown HRF is estimated by fitting a GLM over the impulse train. Using this HRF, the stimulus signal estimation is updated by applying a Wiener filter. For the same task, [10] utilizes a two-step optimization approach that sequentially updates the stimulus signal and predicted HRF. However, both approaches are presented for one-dimensional data, which means either a single voxel or the average response of a region of interest (ROI) can be analyzed and any mutual information that can be shared among various voxels is lost. On the other hand, with multi-dimensional processing methods based on instantaneous mixtures such as independent component analysis which models the measurement signals as linear combinations of

several sources, the extracted source signals still need to be deconvolved into HRFs and stimulus signals [11].

Convolutive mixtures provide a multiple-input-multiple-output setting through convolutive mixing filters (HRFs) which relate multiple input signals (sources or stimuli) to multiple observations (voxel measurements). The characteristics of convolutive mixing filters depend on the source type and measurement number, which allows capturing of the HRF variability across different brain regions and events. Due to their flexibility, convolutive mixtures are used in various applications including audio, image and biomedical signal processing and telecommunications [12]. We propose to model fUS recordings as convolutive mixtures and assume very little prior information, namely that the shape of the HRFs can be parametrized and that the source signals are uncorrelated. Considering the flexibility of tensor-based models while representing such constraints that exist in different modes or factors of data [13], we solve the blind deconvolution problem by applying block-term decomposition (BTD) on the tensor of lagged measurement autocorrelation matrices.

2. PROBLEM FORMULATION

A convolutive mixture of R time-varying sources $s_r(t) \in \mathbb{R}^N, r = 1, 2, \ldots, R$ detected in M measurements $y_m(t) \in \mathbb{R}^N, m = 1, 2, \ldots, M$ can be written as

$$y_m(t) = \sum_{r=1}^{R} \sum_{l=0}^{L} h_{mr}(l) s_r(t-l) \tag{1}$$

where $h_{mr}(l)$ is the convolutive mixing filter of length $L+1$, belonging to the measurement m and source r [14]. The convolutive mixing filter can be considered as an extension of an LTI filter by introducing the mixing effect of multiple sources.

In the context of fUS, each m corresponds to a voxel. Some of the sources are task-related (T), corresponding to the stimuli of the experiment. Such sources are expected to be convolved with an HRF. On the other hand, the rest of the sources, which are artifact-related (A), are directly additive on the measurements [15]. To incorporate this in Eq. 1, each $h_{mr}(l)$ with $r \in A$ should correspond to a unit impulse function. Thus, we rewrite Eq. 1 as:

$$\begin{aligned} y_m(t) &= \sum_{r\in T} \sum_{l=0}^{L} h_{mr}(l) s_r(t-l) + \sum_{r\in A} \sum_{l=0}^{L} \delta(l) s_r(t-l) \\ &= \sum_{r\in T} \sum_{l=0}^{L} h_{mr}(l) s_r(t-l) + \sum_{r\in A} s_r(t). \end{aligned} \tag{2}$$

We aim at solving the blind deconvolution problem to recover the source signals of interest ($s_r, r \in T$) and the corresponding HRFs ($h_{mr}, r \in T$) distinctly for each voxel m.

3. PROPOSED METHOD

We start by expressing the convolutive mixtures formulation in Eq. 1 in matrix form as $\mathbf{Y} = \mathbf{HS}$. The columns of $\mathbf{Y}$, and $\mathbf{S}$ are given as $\mathbf{y}(n), n = 1, \ldots, N - L'$ and $\mathbf{s}(n), n = 1, \ldots, N - (L + L')$, respectively. These column vectors are constructed by selecting the samples of measurement and source signals as follows [16]:

$$\begin{aligned} \mathbf{y}(n) = [&y_1(n), ..., y_1(n - L' + 1), \\ &..., y_M(n), ..., y_M(n - L' + 1)]^T \text{ and} \\ \mathbf{s}(n) = [&s_1(n), ..., s_1(n - (L + L') + 1), \\ &..., s_R(n), ..., s_R(n - (L + L') + 1)]^T \end{aligned} \tag{3}$$

where L' is chosen such that $ML' \geq R(L + L')$. Note that both $\mathbf{Y}$ and $\mathbf{S}$ consists of Hankel blocks.

The mixing matrix $\mathbf{H}$ is equal to

$$\mathbf{H} = [\mathbf{H}_1 \quad \ldots \quad \mathbf{H}_R] = \begin{bmatrix} \mathbf{H_{11}} & \ldots & \mathbf{H_{1R}} \\ \vdots & \ddots & \vdots \\ \mathbf{H_{M1}} & \ldots & \mathbf{H_{MR}} \end{bmatrix} \tag{4}$$

whose any block-entry $\mathbf{H}_{mr}$ is the Toeplitz matrix of $h_{mr}(l)$:

$$\mathbf{H}_{mr} = \begin{bmatrix} h_{mr}(0) & \ldots & h_{mr}(L) & \ldots & 0 \\ & \ddots & \ddots & \ddots & \\ 0 & \ldots & h_{mr}(0) & \ldots & h_{mr}(L) \end{bmatrix}. \tag{5}$$

Next, the autocorrelation $\mathbf{R_y}(\tau)$ for a time lag τ is expressed as:

$$\begin{aligned} \mathbf{R_y}(\tau) &= \mathrm{E}\{\mathbf{y}(n)\mathbf{y}(n+\tau)^T\} = \mathrm{E}\{\mathbf{Hs}(n)\mathbf{s}(n+\tau)^T\mathbf{H}^T\} \\ &= \mathbf{H}\mathbf{R_s}(\tau)\mathbf{H}^T, \quad \forall\tau. \end{aligned} \tag{6}$$

The lagged output autocorrelation matrices $\mathbf{R_y}(\tau)$ are stacked for all τ values to obtain a tensor $\boldsymbol{\mathcal{T}}$ which gives rise to the decomposition shown in Fig. 1 following Eq. 6. Note that, due to the Hankel-block structure of $\mathbf{Y}$ and $\mathbf{S}$, $\mathbf{R_y}(\tau)$ and $\mathbf{R_s}(\tau)$ are Toeplitz-block matrices. Furthermore, assuming that the sources are uncorrelated, $\mathbf{R_s}(\tau)$'s should also be block-diagonal, i.e. non-block-diagonal terms representing the correlations between different sources should be 0. This assumption leads to a unique BTD known as $(L+L', L+L', \cdot)$-BTD. In general, a BTD approximates a tensor by a sum of low multilinear rank terms, which for the given case all carry a rank of $(L + L', L + L', \cdot)$ [17].

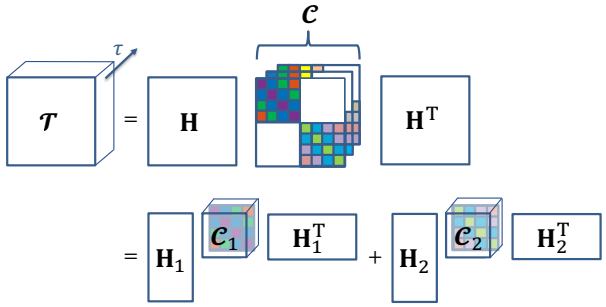

Fig. 1: A demonstration of BTD for $R = 2$. The tensor $\boldsymbol{\mathcal{T}}$ of stacked voxel autocorrelations $\mathbf{R_y}(\tau)$, $\forall\tau$ is first expressed in terms of the mixing matrix $\mathbf{H}$ and a core tensor $\boldsymbol{\mathcal{C}}$ which shows the stacked source autocorrelations $\mathbf{R_s}(\tau)$, $\forall\tau$. Each $\mathbf{R_s}(\tau)$ corresponds to a frontal slice of $\boldsymbol{\mathcal{C}}$ and exhibits a block-diagonal structure with Toeplitz-blocks. $\boldsymbol{\mathcal{T}}$ is decomposed into $R = 2$ terms, each of which contains a core tensor ($\boldsymbol{\mathcal{C}}_1$ or $\boldsymbol{\mathcal{C}}_2$, which represents the autocorrelation of the corresponding source) and a block column of $\mathbf{H}$ ($\mathbf{H}_1$ or $\mathbf{H}_2$).

The solution provided so far has been for the general case of convolutive mixtures. Considering our signal model where we separate the signal subspace from the noise subspace (Eq. 2), we write $\mathbf{S} = [\mathbf{S}_T \ \mathbf{S}_A]^{\mathrm{T}}$ where $\mathbf{S}_T$ and $\mathbf{S}_A$ shows the sources of interest and artifact sources respectively. Similarly, $\mathbf{H} = [\mathbf{H}_T \ \mathbf{H}_\delta]$ where $\mathbf{H}_T$ stands for the block columns of $\mathbf{H}$ that are of interest (i.e., contains the HRFs) and $\mathbf{H}_\delta$ denotes the artifact-related block columns of $\mathbf{H}$, whose subscript δ is used to emphasize that the block

entries of such columns are constant and constructed using filters $h_{mr}(l) = \delta(l)\ \forall m$. That being the case, relative scaling of artifact sources at each voxel is currently not accommodated in the model, i.e. we assume that the artifacts affect each voxel at the same extent.

In addition, a shape constraint is applied to the HRFs such that they are physiologically interpretable. HRFs are most commonly expressed as the difference of two gamma functions [18] and depend on a set of parameters $\boldsymbol{\theta}$:

$$f(t, \boldsymbol{\theta}) = \theta_1(\Gamma(\theta_2)^{-1}\theta_3^{\theta_2} t^{\theta_2 - 1}\mathrm{e}^{-\theta_3 \mathrm{t}} - \theta_4\Gamma(\theta_5)^{-1}\theta_6^{\theta_5}\mathrm{t}^{\theta_5 - 1}\mathrm{e}^{-\theta_6 \mathrm{t}}). \tag{7}$$

where θ_1 is the scaling parameter to account for the strength of an HRF and the rest of the parameters define the shape of the HRF.

Finally, the BTD is computed by minimizing the cost function:

$$J(\boldsymbol{\mathcal{C}}, \boldsymbol{\theta}) = \|\boldsymbol{\mathcal{T}} - \sum_{r \in T} \boldsymbol{\mathcal{C}}_r \times_1 \mathbf{H}_r(\boldsymbol{\theta}_r) \times_2 \mathbf{H}_r(\boldsymbol{\theta}_r) - \sum_{r \in A} \boldsymbol{\mathcal{C}}_r \times_1 \mathbf{H}_\delta \times_2 \mathbf{H}_\delta\|_F^2 \tag{8}$$

while all $\mathbf{H}_r$'s and $\boldsymbol{\mathcal{C}}_r$'s are structured to have Toeplitz blocks. The operator $||\cdot||_F$ is the Frobenius norm. The BTD is implemented using the structured data fusion (SDF) framework, more specifically using the quasi-Newton algorithm `sdf_minf`, offered by Tensorlab [19] with 50 iterations.

The optimal parameters $\hat{\boldsymbol{\theta}}_r$ calculated via Eq. 8 determine the predicted HRFs and thus $\hat{\mathbf{H}}_T = [\mathbf{H}_r(\hat{\boldsymbol{\theta}}_r)]_{r \in T}$. Finally, the task-related sources are recovered by:

$$\hat{\mathbf{S}}_T = \hat{\mathbf{H}}_T^{\dagger}\mathbf{Y} \tag{9}$$

where $(.)^{\dagger}$ shows the Moore-Penrose pseudo-inverse.

Truncated singular value decomposition is a common method used for calculating the pseudo-inverse of a matrix that is rank deficient, which is the case for many signal processing applications including extraction of signals from noisy environments [20]. We follow this approach and set the singular values of $\hat{\mathbf{H}}_T$ that are below a tolerance value to 0. Although currently the tolerance is determined heuristically, this selection can be automated using an appropriate model selection approach [21].

4. SIMULATION RESULTS

In simulations, we assume that there are two sources and three voxels. One of the sources stands for the artifacts such as subject motion and modeled in accordance with [22]. The second source is a binary vector (equal to 1 during a task and 0 during rest) representing the stimulus. The stimulus paradigm, which will also be used in experiments with the mouse, consists of varying task (0.25,0.5,1,2,...,10 s) and rest ([20-25] s) durations in order to observe the response of the mouse under different stimulus conditions and suppress the habituation of the mouse respectively. The stimulus is later convolved with an HRF and the artifact source is directly added to the result of the convolution to construct the measurement signal of a voxel. We assumed that the HRF is the same for the first two voxels and different for the third in order to check if the proposed method is able to capture both the similarities and differences of HRFs.

The results are provided in Fig. 2. The estimated HRFs, stimulus and measurement signals reveal a significant resemblance with the actual versions. In addition, the performance of the proposed method is shown to be robust against noise when evaluated against different signal-to-noise ratio (SNR) values using the Pearson correlation coefficient between the recovered and original stimulus signal.

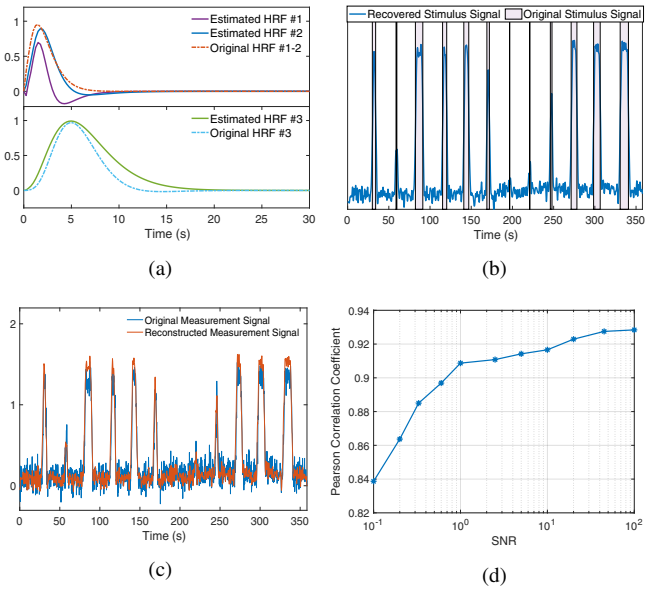

Fig. 2: Simulation results. Predicted HRFs (a), stimulus (b) and measurement (for one voxel) (c) signals are shown under an SNR value of 10. The change in the correlation between the original and reconstructed stimulus with respect to SNR is shown in (d).

5. EXPERIMENTAL RESULTS

The experimental setup is shown in Fig. 3. During data acquisition, 14 tilted plane waves are transmitted from the ultrasonic transducer which is placed on the cranial window of the mouse. After Fourier-domain beamforming and angular compounding of the echo waves, singular value decomposition-based clutter filtering [23] is utilized to remove the tissue echoes. Finally, 120 compound images are used to compute one power-Doppler image. Each voxel is temporally normalized and low-pass filtered at a cut-off frequency of 0.2 Hz.

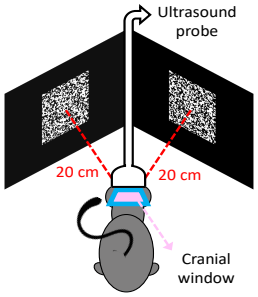

Fig. 3: Experimental setup.

The visual stimulus paradigm is the same as in simulations where the task periods are determined by displaying high-contrast images on two screens placed in front of the mouse. Note that we intentionally chose a setting where we know the actual stimulus onsets to validate our source estimation. However, in many important neuroscience applications including rather spontaneous events, stimuli will be unknown, such as in the case of detection of epileptic seizures.

To determine the regions that are involved in processing of the stimulus, the correlation image provided in Fig. 4a is obtained by

correlating each voxel time-series with a delayed version of the stimulus (the optimal amount of delay is adjusted as the one producing the highest correlation value). Two voxels are selected from a highly-correlated region around superior colliculus (SC) and a third voxel is selected from a relatively poorly-correlated region, near primary visual cortex (V1). We assume there are two sources.

The results of HRF estimation in both regions point out an earlier peak response than the canonical model (Fig. 4b), which was expected as the changes in blood oxygenation have been reported to lag those in blood flow and volume [24]. Furthermore, the estimated HRFs in SC carry a similar time-to-peak that is observed to be preceding the HRF estimated in V1 by approximately 1 second, which is again consistent with prior studies [25].

Reconstructed stimulus signals are shown in Fig. 5. Note that due to high noise contribution in the real data, we only considered two singular vectors while solving Eq. 9, which produces smooth stimulus signal estimations. We compare the proposed method with the BTD solution where only the scaling parameters (θ_1 in Eq. 7) of HRFs are estimated whereas the shape of all HRFs are assumed constant according to the canonical model. With fewer parameters to be estimated, the problem then becomes easier to solve, yet at the cost of ignoring probable variations in the shape of HRFs. The correlation coefficient between the recovered and original stimulus signal is 0.7 with the proposed method and 0.67 with only scaling estimation.

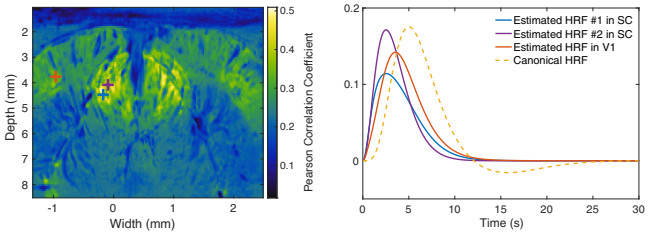

(a) (b)

Fig. 4: Selected voxels (a) (two from SC and one from V1) with the corresponding HRF estimations (b).

6. DISCUSSION

The stimulus estimation results reveal that varying only the scaling of HRFs leads to more shifting of peaks (local maxima, i.e. data samples that are greater than their two neighboring samples) and in general a higher number of peaks than the actual stimulus signal has. The extra peaks and peaks that appear before the actual stimulus onsets (such as around the 50^{th} second) are observed to be particularly concentrated around short stimulus durations. The results of [25] show that HRF peaks especially faster for shorter visual stimuli, and assuming that is the case, the fixed and relatively slow peak of the canonical model might cause the peaks of the recovered stimulus signal to appear differently than expected. On the other hand, the proposed method provides a less noisy estimation of the stimulus signal, and all-but-one of its peaks fall into the actual task periods.

The presented approach performs blind deconvolution with the help of very little prior information. This constitutes a severely ill-posed problem and results in a vast amount of possible solutions. In order to provide more guidance and limit the range of these solutions, gamma-model parameters defining the HRF shapes can be bounded to a priori determined intervals [10] or can be subject to

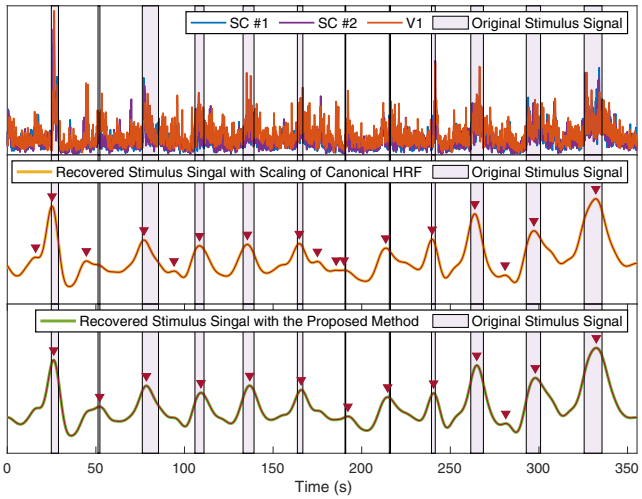

Fig. 5: Acquired measurement signals (top row), from which the original stimulus signal is recovered with scaling estimation of the canonical model (middle row) and the proposed method (bottom row).

spatial regularization. It is known that HRF changes smoothly across brain regions, which means that the parameters of neighboring voxels should be similar [26]. Furthermore, the effect of HRF mismodeling (e.g. when a fixed shape is assumed) will have a stronger impact on the deconvolution in case of event-related experimental designs which incorporate much shorter stimulus durations, making proper HRF estimation even more important.

7. CONCLUSION

We proposed to model fUS measurements as convolutive mixtures for the problem of jointly estimating HRFs and stimuli. Based on the second-order statistics of lagged output autocorrelation matrices, a tensor-based solution is used for the blind deconvolution problem. The proposed method is shown to be robust against noise in simulations and provided meaningful results on real data. In the future, we aim to extend our approach for various experimental paradigms and brain regions while taking into account prior information on neurosignals by means of spatial regularization.

8. REFERENCES

[1] S. Soloukey *et al.*, "Functional ultrasound during awake brain surgery: The clinical potential of intra-operative functional and vascular brain mapping," *Frontiers in Neuroscience*, vol. 13, p. 1384, 2020.

[2] K. J. Friston *et al.*, "Event-related fmri: Characterizing differential responses," *NeuroImage*, vol. 7, pp. 30–40, 1998.

[3] D. A. Handwerker *et al.*, "Variation of bold hemodynamic responses across subjects and brain regions and their effects on statistical analyses," *NeuroImage*, vol. 21, no. 4, pp. 1639 – 1651, 2004.

[4] M. Lindquist *et al.*, "Modeling the hemodynamic response function in fMRI: Efficiency, bias and mis-modeling," *NeuroImage*, vol. 45, pp. S187–98, 12 2008.

[5] G. Glover, "Deconvolution of impulse response in event-related bold fmri1," *NeuroImage*, vol. 9, pp. 416–429, 1999.

[6] C. Liang *et al.*, "Luminance contrast of visual stimulus modulates the bold response more than the cerebral blood flow response in the human brain," *NeuroImage*, vol. 64C, pp. 104–111, 09 2012.

[7] C. C. Gaudes *et al.*, "Detection and characterization of single-trial fmri bold responses: Paradigm free mapping," *Human Brain Mapping*, vol. 32, 2011.

[8] F. I. Karahanoglu *et al.*, "Total activation: fmri deconvolution through spatio-temporal regularization," *NeuroImage*, vol. 73, pp. 121–134, 2013.

[9] G.-R. Wu *et al.*, "A blind deconvolution approach to recover effective connectivity brain networks from resting state fmri data," *Medical image analysis*, vol. 17, 01 2013.

[10] H. Cherkaoui *et al.*, "Sparsity-based blind deconvolution of neural activation signal in fmri," in *ICASSP 2019 - 2019 IEEE International Conference on Acoustics, Speech and Signal Processing (ICASSP)*, 2019, pp. 1323–1327.

[11] F. Moeller, P. LeVan, and J. Gotman, "Independent component analysis (ica) of generalized spike wave discharges in fmri: Comparison with general linear model-based eeg-fmri," *Human brain mapping*, vol. 32, pp. 209–17, 02 2011.

[12] X.-F. Xu *et al.*, "Convolutive blind source separation based on joint block toeplitzation and block-inner diagonalization," *Signal Processing*, vol. 90, pp. 119–133, 01 2010.

[13] L. Sorber, M. Van Barel, and L. De Lathauwer, "Structured data fusion," *IEEE Journal of Selected Topics in Signal Processing*, vol. 9, no. 4, pp. 586–600, 2015.

[14] M. S. Pedersen *et al.*, "A survey of convolutive blind source separation methods," in *Springer Handbook of Speech Processing*. Springer Press, Nov 2007.

[15] G. Marrelec *et al.*, "Robust bayesian estimation of the hemodynamic response function in event-related bold fMRI using basic physiological information," *Human brain mapping*, vol. 19, pp. 1–17, 06 2003.

[16] H. Bousbia-Salah *et al.*, "Jacobi-like algorithm for blind signal separation of convolutive mixtures," *Electronics Letters*, vol. 37, pp. 1049 – 1050, 09 2001.

[17] F. V. Eeghem and L. D. Lathauwer, "Second-order tensor-based convolutive ICA: Deconvolution versus tensorization," *2017 IEEE International Conference on Acoustics, Speech and Signal Processing (ICASSP)*, pp. 2252–2256, 2017.

[18] S. Van Eyndhoven *et al.*, "Flexible fusion of electroencephalography and functional magnetic resonance imaging: Revealing neural-hemodynamic coupling through structured matrix-tensor factorization," in *2017 25th European Signal Processing Conference (EUSIPCO)*, 2017, pp. 26–30.

[19] N. Vervliet *et al.* (2016, Mar.) Tensorlab 3.0. Available online. [Online]. Available: https://www.tensorlab.net

[20] J. W. Demmel, *Applied Numerical Linear Algebra*. USA: Society for Industrial and Applied Mathematics, 1997.

[21] Myung, "The importance of complexity in model selection." *Journal of mathematical psychology*, vol. 44 1, pp. 190–204, 2000.

[22] N. Correa *et al.*, "Comparison of blind source separation algorithms for fMRI using a new matlab toolbox: Gift," in *Proceedings. (ICASSP '05). IEEE International Conference on Acoustics, Speech, and Signal Processing, 2005.*, vol. 5, 2005, pp. v/401–v/404 Vol. 5.

[23] C. Demené *et al.*, "Spatiotemporal clutter filtering of ultrafast ultrasound data highly increases doppler and fultrasound sensitivity," *IEEE Transactions on Medical Imaging*, vol. 34, no. 11, pp. 2271–2285, 2015.

[24] Y. Hirano *et al.*, "Investigation of the bold and cbv fMRI responses to somatosensory stimulation in awake marmosets," *NMR in Biomedicine*, vol. 31, p. e3864, 12 2017.

[25] L. Lewis *et al.*, "Stimulus-dependent hemodynamic response timing across the human subcortical-cortical visual pathway identified through high spatiotemporal resolution 7t fmri," *NeuroImage*, vol. 181, 06 2018.

[26] F. Miezin *et al.*, "Characterizing the hemodynamic response: Effects of presentation rate, sampling procedure, and the possibility of ordering brain activity based on relative timing," *NeuroImage*, vol. 11, pp. 735–59, 07 2000.